Abstract for the 37h AIAA Thermophysics Conference ,June 28-July1, 2004 , Portland, OR.

Aerothermal Performance Constraint Analysis of Sharp Nosecaps and Leading Edges

Yehia Rizk and Ken Gee
NASA Ames Research Center

Objective

The main objective of this work is to predict the Aerothermal Performance Constraint (APC) for a class of Crew Transfer Vehicles (CTV) with shap noses and wing leading edges made out of UHTC which is a family of Ultra High Temperature Ceramics materials developed at NASA Ames. The APC is based on the theoretical temperature limit of the material which is usually encountered at the CTV nose or wing leading edge. The APC places a lower limit on the trajectory of the CTV in the altitude velocity space. The APC is used as one of the constraints in developing reentry and abort trajectories for the CTV. The trajectories are then used to generate transient thermal response of the nosecaps and wing leading edges which are represented as either a one piece of UHTC or two piece (UHTC + RCC) with perfect axial contact. The final paper will include more details about the analysis procedure and will also include results for reentry and abort design trajectories.

Analysis Procedure

The aerothermal analysis at zero angle of attack was performed using the Engineering Method to compute the convective heating . For non-zero angles of attack, the GASP code was used at relatively low altitudes and a non-continuum Direct Simulation Monte Carlo (DSMC) code was used at relatively high altitudes where the Knudsen number Kn > 0.1.

Both steady state and transient thermal analysis were performed using the ANSYS code which accounts for indepth heat conduction and surface heat radiation.

Preliminary Results

Geometry and Angle of attack effects Analysis was performed for the CTV nose and wing leading edge. The nose was modeled either like a wedge or a cone while the flow normal to the wing LE was assumed to be two-dimensional and the wing was modeled as a 2D airfoil. For the configurations considered, it was found that the APC is restricted by the nose geometry and not the wing LE

as shown in Fig. 1. The figure also shows the effects of the angle of attack on the APC for a one piece material.

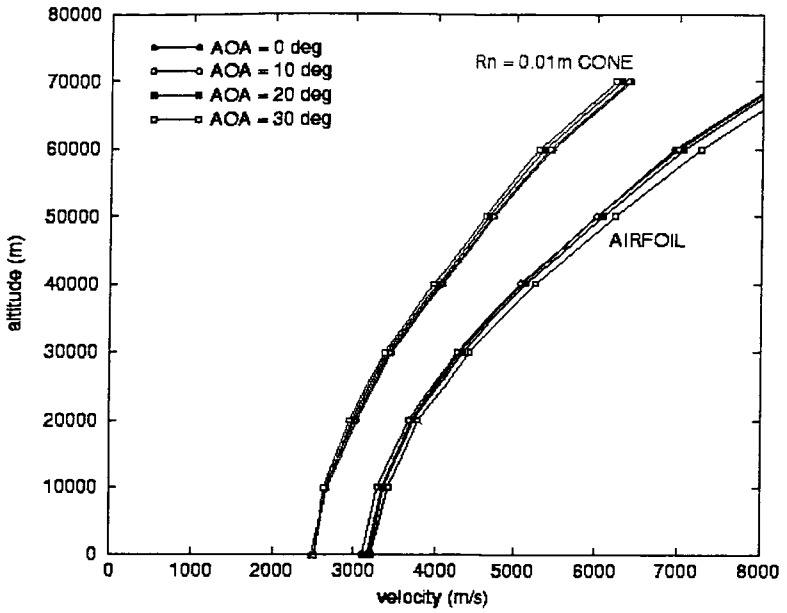

Figure 1. Effect of angle of attack on the APC for the nose cone and the wing leading edge airfoil for CTV

One-piece Vs. two-piece material Comparison between one piece of UHTC and two piece material (UHTC + RCC) showed that there is no noticeable change in the APC as long as the length of the front UHTC piece (Xsplit) is longer than 0.04 m (for a cone with a radius of 0.01 m) as shown in Fig. 2. If the UHTC piece is shorter than .04 m, the APC becomes more restrictive due to the temperature limit in the trailing RCC piece

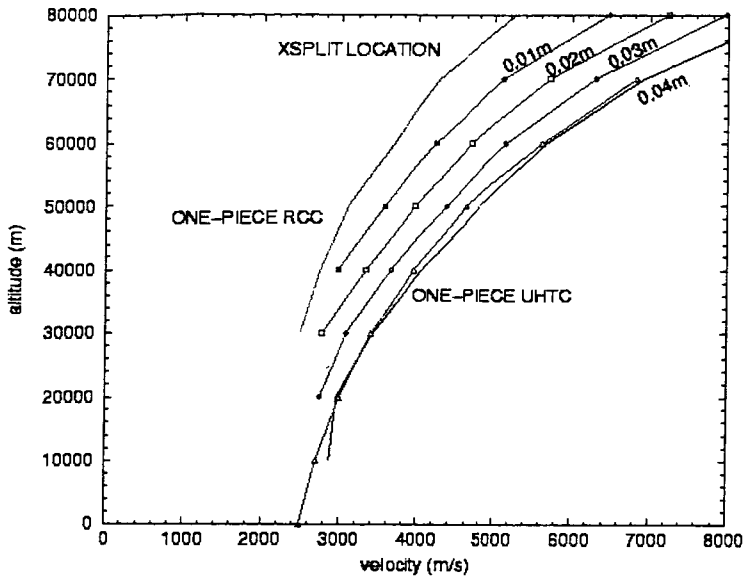

Figure 2. Effect of Xsplit on APC curves for a 2 piece cone with Rn = 0.01m

Effect of AOA on Two-piece material The effect of angle of attack on a typical internal temperature distribution for a two piece wedge with Rn = 0.01m is shown in Figure 3 for an angle of attack of 20 degrees and in Figure 4 for an angle of attack of 40 degrees. With an increase in angle of attack the second piece temperature increases on the windward side. This indicates that the optimum split line location at which the RCC temperature limit is the constraint will increase with an increase in the angle of attack.

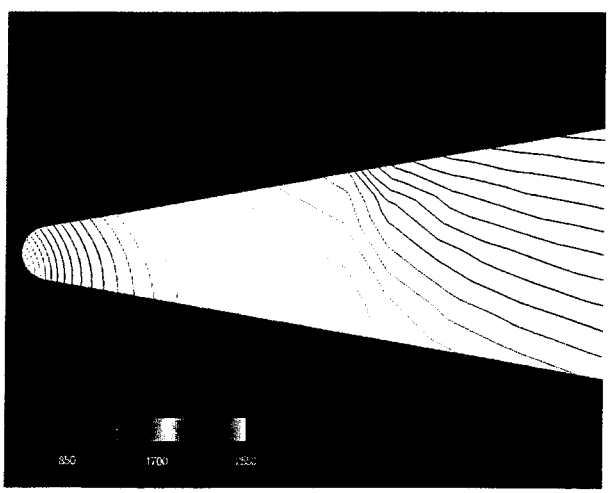

Figure 3. Internal steady state temperature contours for two piece at 20 deg. angle of attack for a wedge with Rn = 0.01m, θ = 10 deg

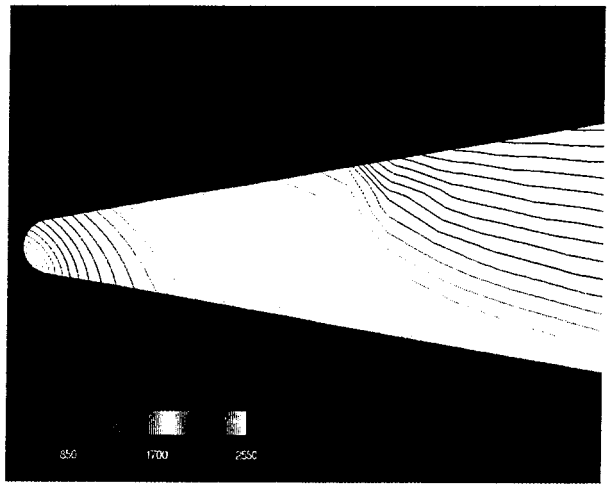

Figure 4. Internal steady state temperature contours for two piece at 40 deg. angle of attack for a wedge with Rn = 0.01m, θ = 10 de

The variation of the optimum split line location with angle of attack in Figure 5. It is seen that the optimum value increases from ~0.06 m at zero angle of attack to ~ 0.10 m at angle of attack of 40 degrees. This indicate that the angle of attack has a major impact on the split line location.

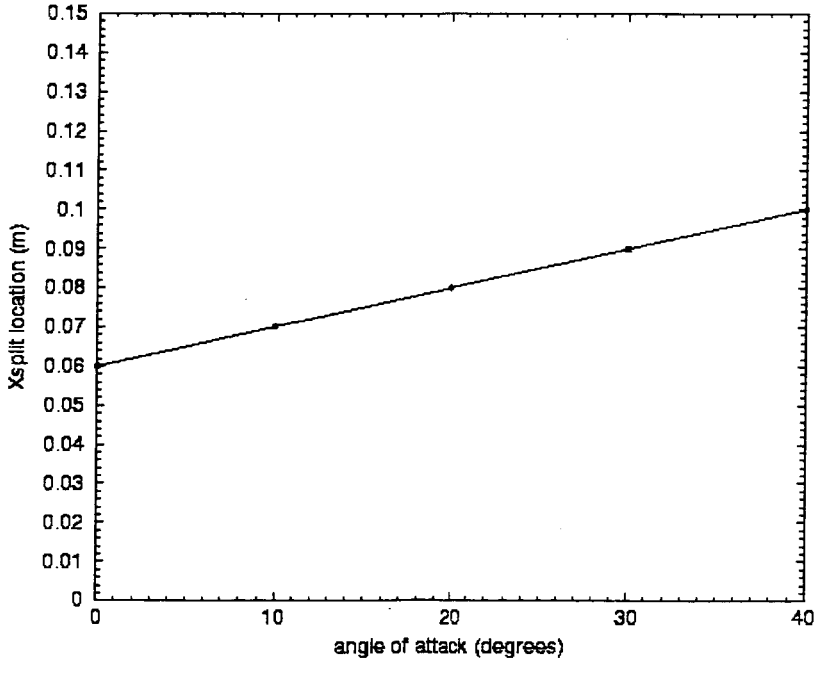

Figure 5. Effect of angle of attack on the optimum value of split line location at altitude of 50 km for a wedge with Rn = 0.01m, θ = 10 deg

In general the optimum split line location will also depend on the geometry (nose radius and wedge half angle) . Also, the optimum split line location depends on the material properties (use temperature, thermal conductivity and emissivity) of the trailing piece and will be given in the final paper.

Transinet Analysis of nominal trajectory The thermal response for the nominal trajectory is plotted in Fig. 6, which shows the maximum temperature in the front and back pieces as a function of time. In the first part of the trajectory, the temperature in the front piece increases at the rate of about 9° K per second until it reaches the theoretical maximum temperature. The temperature then stays close to the theoretical maximum temperature for about 8 minutes. The LE then cools at the rate of about 7° K per second when the CTV trajectory jumps off the APC to satisfy the g-load constraint..

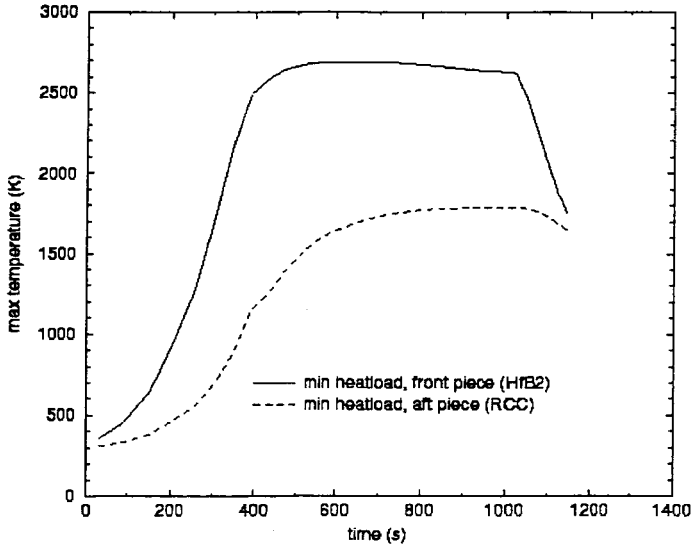

Figure 6. Thermal response of front and back pieces for Min. heat load trajectory

In order to understand the effect of the time step on the transient analysis, the thermal response was performed using a time step of 30 seconds and a time step of 60 seconds. A comparison between the resulting thermal responses is given in Fig. 7. It is seen that there is no significant change in the thermal responses between the 30 sec and 60 sec time steps. Based on that, the time step used in all the current analysis was 60 seconds or less.

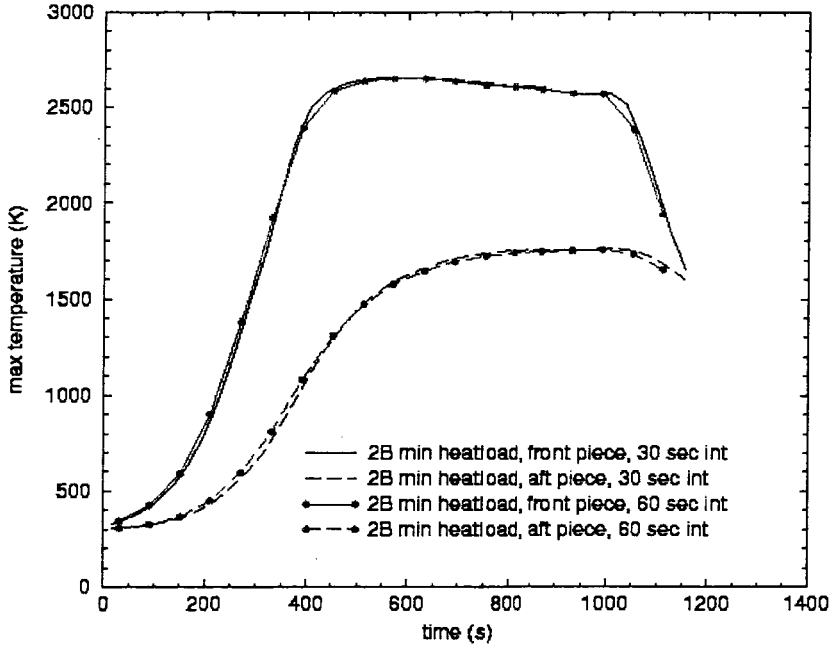

Figure 7. Effect of time step on thermal response of front and back pieces.